

environmentally sound AFFF disposal technologies makes it difficult to safely arrange for the disposal of stockpiled AFFF; and (2) heavily contaminated soils that have the potential to leach PFASs into groundwater creating a public health hazard. Such issues are further compounded by the wide range of AFFF formulations that have been used over several decades, with these AFFF concentrates comprising varying proportions of proprietary PFASs, solvents, and other surfactants.¹¹

The exact composition of any given AFFF product is protected, usually by patents, product trademarks, and trade-secrets.¹² In most cases, the ambiguous 'fluorosurfactant' classification that appears on AFFF manufacturer labels are largely precursor substances that transform into recalcitrant PFASs within the environment. For example, precursor compounds commonly used in historic AFFF concentrate formulations included 8:2 fluorotelomer alcohol and perfluorooctane sulfonamide which can transform to perfluorooctanoic acid (PFOA) and perfluorooctane sulfonic acid (PFOS), respectively.¹³ Additional PFAS precursor subgroups include fluorotelomer sulfonates (FTSs), fluorotelomer sulfonamide betaines, fluorotelomer sulfonamide amines, and other per- or polyfluorinated compounds.^{9,11,14} Therefore, AFFF-contaminated sites typically have a wide variety of PFASs present in the soil and groundwater, some of which have transformed biotically or abiotically into their environmentally-stable 'end-products' that cannot be broken down further by natural processes (*e.g.*, PFOA, PFOS).^{9,14} For these reasons, suitable destruction technologies for PFASs in AFFF products or AFFF-impacted matrices must have the capability to destroy the sum total of PFASs due to the presence of unknown precursors in AFFF products, as well as environmentally persistent end-products in AFFF-impacted soil.

We have recently studied the degradation of perfluorosulfonic acid (PFSA) standards under mechanochemical destruction (MCD) conditions on quartz sand, which highlighted the radical-mediated degradation pathway of these compounds ultimately resulting in the formation of stable Si-F bonds embedded in the silica matrix.¹⁵ Other studies have also established the effectiveness of MCD to destroy a variety of topical persistent PFASs under laboratory conditions.^{16–21} This degradative phenomenon can be explained by the mechanical activation of the matrix and the generation of highly reactive surface sites on freshly formed surfaces which initiate and propagate the mineralisation of organic substances, such as PFASs.^{22–25}

To the best of our knowledge, there are only three available studies where researchers demonstrated the ability of the MCD technique to destroy PFASs in real-world contaminated soils^{26,27} or sediments.²⁸ All three studies used potassium hydroxide (KOH) to enhance PFAS destruction during MCD treatment, with one group using the piezoelectric material, boron nitride (BN). It should be noted that using KOH as a grinding agent for PFAS-impacted solids will likely lead to detrimental side-effects when establishing scale-up parameters: the MCD process is known to generate harmful potassium fluoride (KF) when KOH is used, and the end product would have a very high pH

requiring specialist handling. It is likely that both KOH and BN would be prohibitively expensive co-milling agents for the treatment of contaminated environmental matrices at any meaningful scale beyond the laboratory.

The principal objective of the research described herein was to carry out a proof-of-concept case study to determine whether the degradative mechanisms observed in previous fundamental research also apply to PFAS-containing products (*e.g.*, AFFF concentrates) and PFAS-impacted solid matrices (*e.g.*, AFFF-contaminated soil), without the use of unfeasible co-milling agents. Furthermore, we are not aware of any targeted studies that apply the MCD technique for the destruction of PFASs in commercial AFFF products as a potentially scalable treatment method for obsolete foam concentrate stockpiles. Hence, there exists significant literature gaps related to the feasibility and technical capability of MCD to treat PFASs in real-world products and impacted matrices.

Materials and methods

Chemicals and reagents

Tridol S3, a commercial C6 AFFF concentrate manufactured by Angus Fire (UK), was sourced from the New Zealand Defence Force (NZDF). High purity quartz sand (99.2% SiO₂) was sourced from Sigma Aldrich for use in AFFF treatment trials. The AFFF-impacted soil was provided by the NZDF, originating from a contaminated military site in regional New Zealand.

Non-targeted analysis of AFFF concentrate

Prior to MCD treatment trials, elementary non-target high resolution mass spectrometry (HRMS) was employed to determine the PFAS/fluorosurfactant component(s) of the AFFF concentrate. The AFFF was dissolved in methanol at 3 $\mu\text{L mL}^{-1}$ and directly infused into a quadrupole time-of-flight (QToF) mass spectrometer. A Bruker MicroTOF-QII system at the University of Auckland was used for qualitative analysis, equipped with ESI and operated in negative ion mode, with a resolution of 20 000. Bruker Data-Analysis software (version 4.1) was used for data processing. The NIST PFAS Suspect List and analytical chemistry literature were used for the screening of suspect ions.^{11,12}

Mechanochemical processing

2.5 mL of the as-received Tridol S3 AFFF concentrate was pipetted directly onto 25 g of quartz sand to prepare a solid mixture for mechanochemical milling. No pre-conditioning of the AFFF concentrate was conducted. The AFFF-quartz sand mixture was placed into a stainless-steel cylindrical milling vessel with an internal volume of 500 cm³. Twenty stainless steel balls (15 mm diameter, 13.5 g each) were also placed into the vessel with the AFFF-spiked quartz sand and sealed with a stainless-steel lid. A Retsch PM100 planetary ball mill (Germany) was used for all mechanochemical experiments. The ball mill rotational speed was set to 425 rpm and operated for various time intervals from 15 minutes up to 1440 minutes. A custom milling program was set to switch the direction of the vessel rotation every 15 minutes for the specified time of the



trial run to avoid caking on the internal walls of the milling vessel. Each data point was generated from a discrete trial run. All experimental runs were conducted under ambient temperature, pressure, and humidity. The overall milling procedure for the AFFF-contaminated soil was similar to the AFFF-quartz sand trials, except that 25 g of dried AFFF-contaminated soil was placed directly into the milling vessel (*i.e.*, pre-mixing with an AFFF concentrate was not required). Additional details are provided in the ESI.†

Targeted analysis of AFFF-spiked quartz sand and PFAS-contaminated soil

Liquid chromatography tandem mass spectrometry (LC-MS/MS) analysis of all samples was conducted by Analytica Laboratories Limited (New Zealand). Samples were extracted for analysis using a method based on EPA method 537.1, ISO 25101, and ASTM method D7968-17a. In summary, 0.1 g of sample was weighed into a 50 mL polypropylene centrifuge tube and 10 mL of 1% ammonia in methanol was added. The solution was sonicated for 60 min, then 0.6 mL of 50% acetic acid in water was added and the solution was sonicated for a further 15 min. After centrifugation, 0.1 mL of the extract was added into a polypropylene high pressure liquid chromatography (HPLC) vial containing 0.9 mL of 50% methanol in water and was analyzed by LC-MS/MS. While other PFASs were almost certainly present in the AFFF concentrate and impacted soil, targeted analysis by LC-MS/MS was deemed to be the most suitable primary analytical technique for this exploratory study as the results quantitatively assessed the degradation of key topical PFASs, including perfluorosulfonic acids (PFSAs), perfluorocarboxylic acids (PFCAs), and FTSS. The PFASs listed on Table S1 of the ESI† were tracked for the determination of the overall PFAS content in the AFFF concentrate and the contaminated soil. Extractable organic fluorine (EOF) analysis was also employed in this work. Further EOF details are provided in the ESI.†

Results and discussion

Destruction efficiencies for PFASs in AFFF spiked onto quartz sand

The general properties of the Tridol S3 AFFF concentrate are shown in Tables S2 and S3 of the ESI.† Tridol S3 is primarily comprised of water, with 1% to 5% PFASs/fluorosurfactants and about 15% to 20% nonfluorinated organic compounds. Prior to commencing the MCD trials, the Tridol S3 was analysed by QToF high resolution mass spectrometry (HRMS) to qualitatively identify the major PFAS components present in the proprietary AFFF concentrate blend. The most abundant compounds were two related PFASs: 6:2 fluoro-olomermercaptoalkylamido sulfonate (FTSAS) and 6:2 FTSAS sulfoxide. These PFASs have been previously identified as major components of various AFFF concentrates, including Tridol S3.^{12,29} 6:2 FTS was detected by both QToF HRMS and LC-MS/MS. The structures of these substances are shown in Fig. 1, and their putative identification is provided in Table S4.† The relative abundance of 6:2 FTS in comparison to its likely

precursor compounds (6:2 FTSAS; 6:2 FTSAS sulfoxide) was approximately 5%. While not quantitative, this indicative value conveys the variable fluorosurfactant content related to the proprietary mixture of the Tridol S3 AFFF concentrate.

LC-MS/MS was used to evaluate the concentration of 35 target PFAS analytes, or analyte groups, in the AFFF-spiked quartz sand samples that were discretely milled up to 1440 min. The three major PFAS subgroups that were identified and quantitatively tracked during the MCD process were FTSS, PFCAs, and PFSAs, with FTSS making up the majority of PFASs detected in the samples.

The sum concentration of target PFASs in the initial sample was 22.72 mg kg⁻¹, increasing to a maximum concentration of 41.96 mg kg⁻¹ in the 60 min sample, as shown in Fig. 2. Once this maximum was reached, rapid degradation of PFASs ensued. Unless otherwise stated, the dashed lines presented in this study are for visualization of degradation curves only. The substantial increase in the total PFAS concentration of target compounds was most likely associated with the degradation of precursor non-target PFASs into target substances which could be quantitatively assessed by LC-MS/MS. For example, the C-S bonds of the functional group heads for 6:2 FTSAS and 6:2 FTSAS sulfoxide in the Tridol S3 were likely cleaved, resulting in the degradation of these substances into 6:2 FTS which could in turn undergo parallel chain shortening reactions, as described in our previous study.¹⁵ The destruction efficiency (DE) of Σ PFAS was 99.99% after 960 min milling time, following approximately first-order kinetics after the initial increase.

The degradation progression of each PFAS subgroup was diverse, though the trend of Σ PFAS degradation was generally followed. The final DEs for each subgroup was 99.99% for FTSS, 99.88% for PFCAs, and 100% for PFSAs. These trends are comparable to the effective destruction rates of PFAS standards observed in our previous study, using a similar mechanochemical setup and procedure.¹⁵

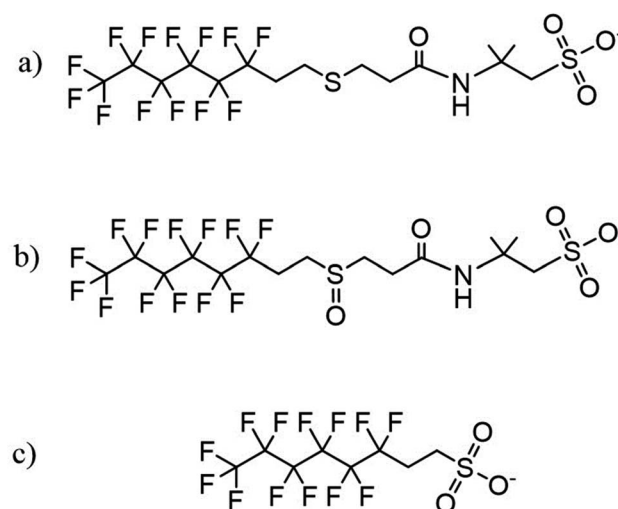


Fig. 1 Structures of PFASs of interest identified in Tridol S3 by QToF HRMS: (a) 6:2 FTSAS, (b) 6:2 FTSAS sulfoxide, and (c) 6:2 FTS.



6 : 2 FTS, which was the most abundant target PFAS in the AFFF concentrate that could be quantitatively tracked, had a DE of 99.99% at the culmination of the milling process (Fig. 3a). 4 : 2 FTS and 8 : 2 FTS were also present in the AFFF concentrate, both achieving a DE of 100% upon extended mechanochemical treatment.

All PFCAs reached a DE of 100% by 960 min, excluding perfluorohexanoic acid (PFHxA) which achieved a maximum DE of 99.82% by 960 min (Fig. 3b). PFOA, PFHxA, perfluoropentanoic acid (PFPeA), and perfluorobutanoic acid (PFBA) had the highest initial PFCa concentrations in Tridol S3. As with the FTS results, PFCAs quickly degraded after reaching their respective maximum concentration (Fig. 3b). Unusually, the concentration of PFHxA, PFPeA, and PFBA increased after 480 min, reaching a maximum concentration at 720 min, followed by degradation. This observation strongly indicates that these PFCAs were intermediate products associated with the degradation of target (*e.g.*, 6 : 2 FTS) and non-target PFAS (*e.g.*, 6 : 2 FTSAS, 6 : 2 FTS sulfoxide).

While only trace concentrations of PFSAs were detected by LC-MS/MS, their inclusion in the overall degradation profile was warranted due to their particularly recalcitrant properties. Both

perfluorohexane sulfonic acid (PFHxS) and PFOS achieved a DE of 100% by 120 min milling time (Fig. 3c). While PFHxS revealed degradation-only kinetics, PFOS showed formation and degradation kinetic progression, suggesting that PFOS was an intermediate product of other non-target precursor PFASs. Larger graphical versions of individual PFAS degradation curves are shown in Fig. S1–S3 of the ESI.†

Overall, the concentration changes of compounds quantified by LC-MS/MS indicated the degradation of target PFASs during MCD treatment. The reproducibility of PFAS destruction was investigated during the preliminary stages of the method development process where replicate samples were milled under identical mechanochemical conditions, achieving destruction efficiencies within a reasonable margin. EOF analysis revealed a 97.8% reduction of non-target PFAS content in the AFFF–quartz sand matrix after MCD treatment (Fig. S4†). While optimization of the MCD technique at benchtop scale was not undertaken as part of this study, this work provides a compelling case for the potential of mechanochemical techniques to address AFFF stockpiles.

As a comparison to the results presented in this work, Battye and colleagues recently conducted MCD experiments that employed significantly lower AFFF spiking concentrations on nepheline syenite sand in order to simulate the capabilities of the MCD technique to process an ‘ideal’ AFFF-impacted matrix.²⁷ It is important to make the distinction that one of the goals of the current study was to carry out AFFF–quartz MCD experiments as part of a higher level proof-of-concept project to determine the feasibility for MCD to treat AFFF stockpiles, not just contaminated matrices with relatively low concentrations of PFASs. When using horizontal ball mills (1 L volume), Battye and co-workers observed comparatively lower destruction rates: the total destruction achieved for 6 : 2 FTS was 23% with no KOH and 91% when KOH was used as a co-milling agent.²⁷ While the exact details of the mechanochemical setup and operating conditions were not disclosed, it is well known that small horizontal ball mills are generally lower energy systems that do not impart the same ball-to-ball and ball-to-surface collision intensities as planetary ball mills.^{30,31} Thus, the

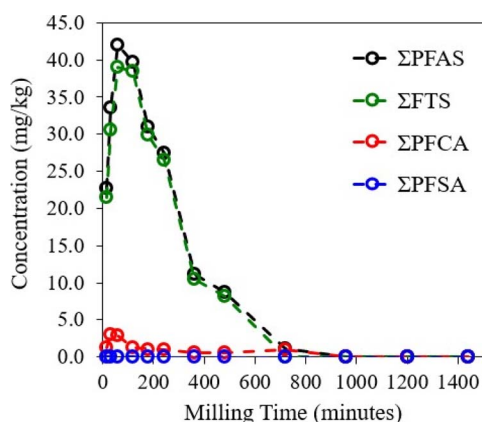


Fig. 2 Degradation curves of Σ PFAS and PFAS subgroups for the AFFF-spiked quartz sand.

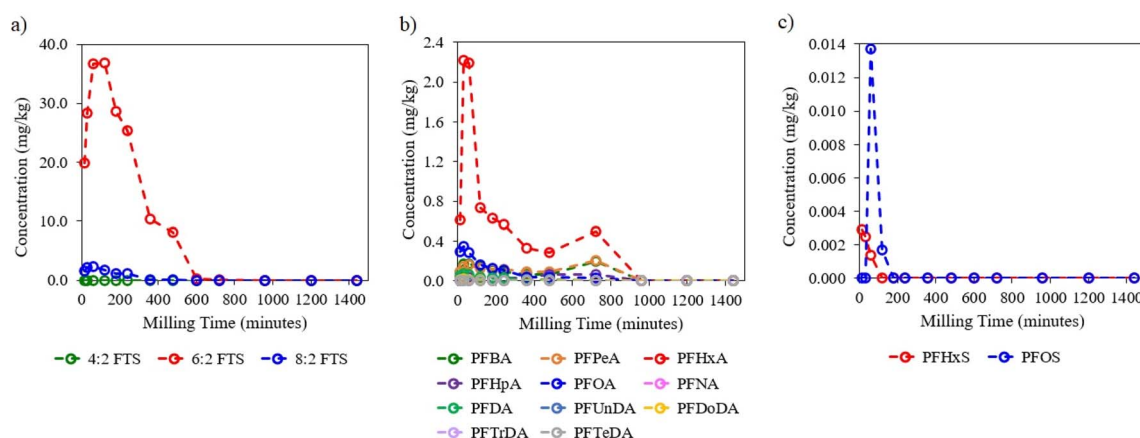


Fig. 3 Degradation curves of target (a) FTSs, (b) PFCAs, and (c) PFSAs determined by LC-MS/MS in the AFFF-spiked quartz sand.



mechanical activation of the solid matrix would have been significantly reduced, which would in turn negatively affect the destruction of target PFAS in the matrix, unless a strong Lewis base (*e.g.*, KOH) was used as a co-milling agent.

The use of quartz sand in the work described herein demonstrates the effectiveness of an easily accessible, inexpensive, and inert co-milling agent for the non-thermal treatment of AFFF concentrate stockpiles. It is envisaged that these results will inform ongoing optimisation research and scale-up activities with suitable industry partners that have developed full-scale mechanochemical systems that impart the requisite intensity of ball-to-ball and ball-to-surface collision points in large continuous-flow vessels.^{23,32,33}

Destruction efficiencies for PFASs in AFFF-contaminated soil

The PFAS-contaminated soil used in this study was derived from a decommissioned NZDF firefighting training facility, comprising a sandy matrix with a low to moderate level of organic matter. An untreated sample was analysed for a general suite of chemical and physical soil properties, shown in Table S5 of the ESI.† The untreated soil was also analysed by LC-MS/MS to determine the starting concentration for each target PFAS which was tracked during subsequent MCD trials. While other organic pollutants were likely present in the sample, these were not included in the analysis. Baseline concentrations revealed that the major PFAS subgroups present in the soil were FTSSs, PFCAs, PFSAs, and perfluoroalkane sulfonamides (FASAs) (Table S6†). This study evaluated the concentration changes of target PFASs in contaminated soil subsamples that were discretely milled up to 1440 min. The degradation curves of total PFAS and the major subgroups are shown in Fig. 4.

The sum concentration of target PFASs in the starting soil sample was initially 0.56 mg kg^{-1} , increasing to a maximum concentration of 0.99 mg kg^{-1} upon 60 min of mechanochemical treatment. In line with the explanation given for the AFFF-spiked quartz sand, the considerable increase in the total PFAS concentration of target compounds was due to the degradation of precursor non-target PFASs into target substances which could be quantified by LC-MS/MS.

The degradation progression of each PFAS subgroup produced variable and irregular concentration curves compared to one another. Nevertheless, all PFAS subgroups were below the limits of detection for the analytical method used in this study by 1440 min mechanochemical treatment.

8 : 2 FTS was the major FTS compound in the AFFF-impacted soil sample. 6 : 2 FTS was also present in the soil sample at significant concentrations, while 4 : 2 FTS was detected at trace concentrations only. The concentration of 8 : 2 FTS and 6 : 2 FTS increased considerably upon 60 min of MCD treatment, after which they both began to slowly degrade before more rapid degradation *via* approximately first-order kinetics (Fig. 5a).

PFCAs followed two distinct reaction progression pathways. The first group revealed initial degradation from 0 min to 240 min followed by a long plateau period up to 960 min, after which these substances were completely degraded (Fig. 5b). The PFCAs in this set comprised short chains like PFBA and PFPeA

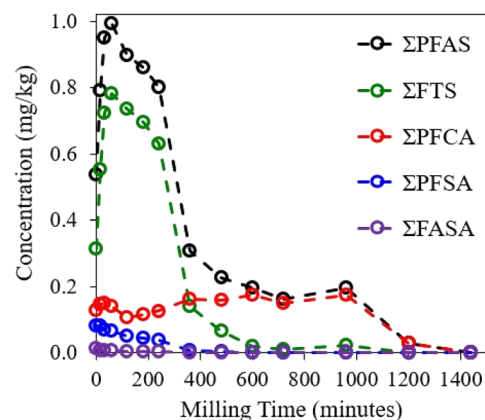


Fig. 4 Degradation curves of Σ PFAS and major PFAS subgroups detected in the milled AFFF-impacted soil samples.

(C4–C5), as well as long chains perfluorodecanoic acid (PFDA), perfluoroundecanoic acid (PFUnDA), perfluorododecanoic acid (PFDoDA), perfluorotridecanoic acid (PFTrDA), and perfluorotetradecanoic acid (PFTeDA) (C10–C14). The second group showed sporadic formation and degradation from 0 min to 120 min then a sustained formation and plateau period up to 960 min, followed by rapid degradation. The PFCAs that fell under this group were PFHxA, perfluoroheptanoic acid (PFHpA), PFOA, and perfluorononanoic acid (PFNA) (C6–C9), which were likely degradation products of non-target precursor compounds of historic AFFFs used at the fire-training site.

Several PFSAs detected in the AFFF-impacted soil sample, with PFOS and PFHxS making up the largest individual components (Fig. 5c). The degradation of PFOS followed roughly first-order degradation kinetics until complete elimination was observed at 600 min. PFHxS only showed sustained degradation from 60 min up to 240 min, at which point it could no longer be detected. Other short chain (C3–C5) and long chain (C9–C10) PFSAs were also detected at trace concentrations in the contaminated soil sample, though these substances were rapidly degraded within 15 min upon exposure to MCD conditions. More detailed graphical versions of individual PFAS degradation curves for FTSSs, PFCAs, and PFSAs in the contaminated soil samples are shown in Fig. S4–S6 of the ESI.†

FASAs were also present at very small concentrations in the contaminated soil sample and revealed degradation-only kinetics upon mechanochemical treatment (Fig. S7†). The inclusion of this subgroup was especially justified due to the detection of perfluorooctane sulfonamide (PFOSA), which is a toxic insecticide and a likely precursor for PFOS, that was completely eliminated by 360 min mechanochemical milling time.

Apart from the trend observed for C6–C9 PFCAs, the general kinetic progression for all other PFASs revealed degradation only reactions once a maximum concentration was observed within the initial 120 minutes of milling. The sand content of the soil likely assisted PFAS destruction, due to the formation of mechanically activated surfaces which facilitate the destruction process of PFASs during mechanochemical treatment.¹⁵



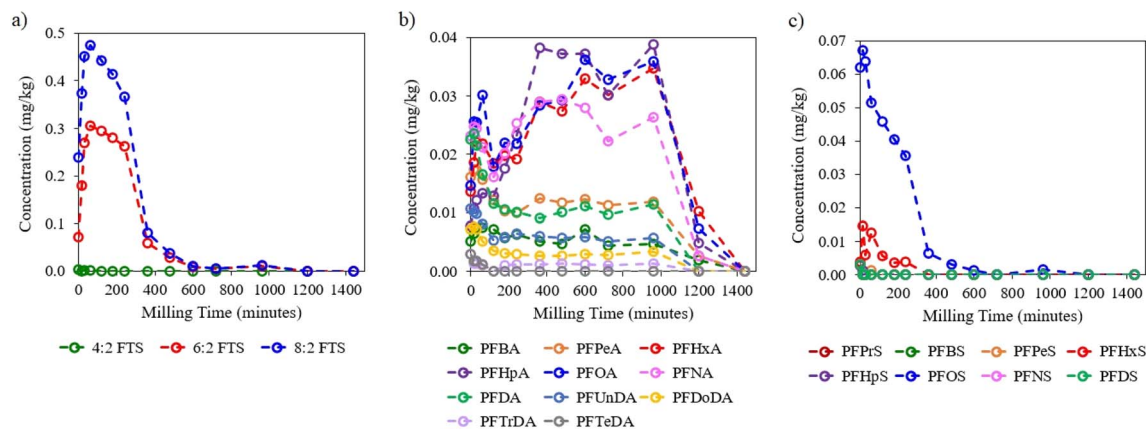


Fig. 5 Degradation curves of target (a) FTSs, (b) PFCAs, and (c) PFASs determined by LC-MS/MS in the AFFF-contaminated soil.

Unlike the Tridol S3 AFFF concentrate, the degradation of PFAS subgroups in the AFFF-contaminated soil was much more complicated, indicating the historic use of multiple AFFFs which contained an array of precursors that have remained in the soil or degraded into more recalcitrant by-products over the years. As with the AFFF concentrate results, LC-MS/MS analysis provided valuable insight into the degradation of target PFASs present in the contaminated soil sample. Employing unoptimized mechanochemical conditions, very positive results were still observed, with EOF analysis revealing a 53.5% reduction of total non-target PFAS content in the contaminated soil sample following MCD treatment (Fig. S9[†]). As an aside, we are currently investigating novel methods for the determination of organic fluorine, with a focus on enhancing sensitivity at low concentrations in environmental media like soil. However, the EOF result found in this study represents double the efficiency of PFAS destruction in comparison to a similar study by Yang and colleagues in which impacted sediment was treated within a planetary ball mill.²⁸

Of particular significance in this work, no co-milling agents (*e.g.*, KOH, boron nitride) were added to the soil prior to MCD treatment, unlike comparable studies.^{26–28} Furthermore, the results observed here revealed higher DEs for a broader range of target PFASs when compared to previous studies that used MCD for the treatment of PFASs in contaminated soils^{26,27} and sediments.²⁸

Conclusions

The observations discussed in this case study highlight two major high level areas of future research and technology development of mechanochemical techniques for the treatment of PFASs in complex solid matrices: (1) utilising a comprehensive targeted and non-targeted analytical regime to provide holistic insight into the degradation of PFASs during MCD treatment, and (2) determining the primary operational variables and matrix properties that influence the destruction of PFASs during MCD treatment, which inherently impacts process scalability.

While assessing the sum total of PFASs in any given sample is subject to analytical issues (*e.g.*, selectivity *versus* inclusivity), the objective of this exploratory work was to provide insight into the degradation of PFASs during MCD treatment. Given the wide range of target analytes, EOF results, and the general trends seen across multiple PFAS subgroups, there is strong evidence to support the destruction PFASs in both the AFFF concentrate and the contaminated soil sample.

Based on the observations described in this study, MCD appears to be an effective treatment technology for PFAS-containing products as well as PFAS-impacted matrices in the presence of sand. The nature of the sand is not essential for the degradation, with sandy soil from the PFAS-impacted soil matrix as effective as the use of purified quartz sand. These results highlight that MCD is an indiscriminate destruction technique for PFASs regardless of variation in functional group, chain length, fluorine saturation, and their relative concentrations in the matrix. Furthermore, this work shows that high rates of PFAS destruction can occur during MCD treatment without the need of impractical co-milling agents, like KOH and BN; both of which were heavily relied upon in previous studies to enhance PFAS destruction. These substances would inherently make scaling the process effectively unfeasible, unlike quartz sand which is easily accessible globally at a low cost. Volatile fluorochemicals were not analysed for, so the complete mineralisation of constituent PFASs could not be confirmed and should be a focus of further studies to ensure that PFASs will not be emitted into the environment and suitable emission capture systems are adequately designed. Further avenues of research should also evaluate the impact of co-contaminants, differences in soil type, and complex PFAS formulations in AFFFs on the optimisation of PFAS destruction (target and non-target) for the treatment of AFFF stockpiles and PFAS-impacted environmental matrices.

Author contributions

Conceptualization: KG, JS, ES, AW; data curation: KG, JS, CCW; formal analysis: KG; funding acquisition: KG, JS; investigation:



KG, JS; methodology: KG, JS, ES, AW, CCW; project administration: KG, JS, ES, AW; resources: KG, JS; validation: KG, JS, ES; visualization: KG, JS; writing – original draft: KG; writing – review & editing: JS, ES, AW, CCW.

Conflicts of interest

There are no conflicts to declare.

Acknowledgements

KG acknowledges the University of Auckland for the award of a University of Auckland Doctoral Scholarship. The views expressed in this article are those of the authors and do not necessarily represent the views or the policies of the U.S. Environmental Protection Agency. Any mention of trade names, manufacturers or products does not imply an endorsement by the United States Government or the U.S. Environmental Protection Agency. EPA and its employees do not endorse any commercial products, services, or enterprises. This document has been reviewed in accordance with U.S. Environmental Protection Agency policy and approved for publication.

References

- 1 J. P. Giesy and K. Kannan, Global distribution of perfluorooctane sulfonate in wildlife, *Environ. Sci. Technol.*, 2001, **35**, 1339–1342.
- 2 A. M. Calafat, L. Y. Wong, Z. Kuklenyik, J. A. Reidy and L. L. Needham, Polyfluoroalkyl chemicals in the U.S. population: data from the national health and nutrition examination survey (NHANES) 2003–2004 and comparisons with NHANES 1999–2000, *Environ. Health Perspect.*, 2007, **115**, 1596–1602.
- 3 J. Glüge, M. Scheringer, I. T. Cousins, J. C. Dewitt, G. Goldenman, D. Herzke, R. Lohmann, C. A. Ng, X. Trier and Z. Wang, An overview of the uses of per- and polyfluoroalkyl substances (PFAS), *Environ. Sci.: Processes Impacts*, 2020, **22**, 2345–2373.
- 4 N. Bolan, B. Sarkar, M. Vithanage, G. Singh, D. C. W. Tsang, H. Li and B. Kirkham, Distribution, behaviour, bioavailability and remediation of poly- and per-fluoroalkyl substances (PFAS) in solid biowastes and biowaste-treated soil, *Environ. Int.*, 2021, **155**, 106600.
- 5 N. Bolan, B. Sarkar, Y. Yan, Q. Li, H. Wijesekara, K. Kannan, D. C. W. Tsang, M. Schauerte, J. Bosch, H. Noll, Y. Sik, K. Scheckel, J. Kumpiene, K. Gobindlal, M. Kah, J. Sperry, M. B. Kirkham, H. Wang, Y. Fai and D. Hou, Remediation of poly- and perfluoroalkyl substances (PFAS) contaminated soils – to mobilize or to immobilize or to degrade?, *J. Haz. Mat.*, 2021, **401**, 123892.
- 6 U.S. EPA, *PFAS Strategic Roadmap: EPA's Commitments to Action 2021–2024*, U.S. EPA, 2021, document EPA-100-K-21-002.
- 7 C. Berg, B. Crone, B. Gullett, M. Higuchi, M. J. Krause, P. M. Lemieux, T. Martin, E. P. Shields, E. Struble, E. Thoma and A. Whitehill, Developing Innovative Treatment Technologies for PFAS-Containing Wastes, *J. Air Waste Manage. Assoc.*, 2021, **72**, 540–555.
- 8 OECD/UNEP, *Toward a New Comprehensive Global Database of Per- and Polyfluoroalkyl Substances (PFASs): Summary Report on Updating the OECD 2007 List of Per- and Polyfluoroalkyl Substances (PFASs)*, 2018.
- 9 A. Nickerson, A. C. Maizel, P. R. Kulkarni, D. T. Adamson, J. J. Kornuc and C. P. Higgins, Enhanced Extraction of AFFF-Associated PFASs from Source Zone Soils, *Environ. Sci. Technol.*, 2020, **54**, 4952–4962.
- 10 W. J. Backe, T. C. Day and J. A. Field, Zwitterionic, cationic, and anionic fluorinated chemicals in aqueous film forming foam formulations and groundwater from U.S. military bases by nonaqueous large-volume injection HPLC-MS/MS, *Environ. Sci. Technol.*, 2013, **47**, 5226–5234.
- 11 R. B. Young, N. E. Pica, H. Sharifan, H. Chen, H. K. Roth, G. T. Blakney, T. Borch, C. P. Higgins, J. J. Kornuc, A. M. McKenna and J. Blotvogel, PFAS Analysis with Ultrahigh Resolution 21T FT-ICR MS: Suspect and Nontargeted Screening with Unrivaled Mass Resolving Power and Accuracy, *Environ. Sci. Technol.*, 2022, **56**, 2455–2465.
- 12 L. A. D'Agostino and S. A. Mabury, Identification of novel fluorinated surfactants in aqueous film forming foams and commercial surfactant concentrates, *Environ. Sci. Technol.*, 2014, **48**, 121–129.
- 13 E. F. Houtz and D. L. Sedlak, Oxidative conversion as a means of detecting precursors to perfluoroalkyl acids in urban runoff, *Environ. Sci. Technol.*, 2012, **46**, 9342–9349.
- 14 H. Chen, M. Liu, G. Munoz, S. V. Duy, S. Sauvé, Y. Yao, H. Sun and J. Liu, Fast Generation of Perfluoroalkyl Acids from Polyfluoroalkyl Amine Oxides in Aerobic Soils, *Environ. Sci. Technol. Lett.*, 2020, **7**, 714–720.
- 15 K. Gobindlal, Z. Zujovic, J. Jaine, C. C. Weber and J. Sperry, Solvent-Free, Ambient Temperature and Pressure Destruction of Perfluorosulfonic Acids under Mechanochemical Conditions: Degradation Intermediates and Fluorine Fate, *Environ. Sci. Technol.*, 2023, **57**, 277–285.
- 16 K. Zhang, J. Huang, G. Yu, Q. Zhang, S. Deng and B. Wang, Destruction of perfluorooctane sulfonate (PFOS) and perfluorooctanoic acid (PFOA) by ball milling, *Environ. Sci. Technol.*, 2013, **47**, 6471–6477.
- 17 K. Zhang, Z. Cao, J. Huang, S. Deng, B. Wang and G. Yu, Mechanochemical destruction of Chinese PFOS alternative F-53B, *Chem. Eng. J.*, 2016, **286**, 387–393.
- 18 N. Wang, H. Lv, Y. Zhou, L. Zhu, Y. Hu, T. Majima and H. Tang, Complete defluorination and mineralization of perfluorooctanoic acid by a mechanochemical method using alumina and persulfate, *Environ. Sci. Technol.*, 2019, **53**, 8302–8313.
- 19 G. Cagnetta, Q. Zhang, J. Huang, M. Lu, B. Wang, Y. Wang, S. Deng and G. Yu, Mechanochemical destruction of perfluorinated pollutants and mechanosynthesis of lanthanum oxyfluoride: A Waste-to-Materials process, *Chem. Eng. J.*, 2017, **316**, 1078–1090.
- 20 M. Lu, G. Cagnetta, K. Zhang, J. Huang and G. Yu, Mechanochemical mineralization of 'very persistent'



- fluorocarbon surfactants –6 : 2 fluorotelomer sulfonate (6 : 2 FTS) as an example, *Sci. Rep.*, 2017, 7, 1–10.
- 21 M. Ateia, L. P. Skala, A. Yang and W. R. Dichtel, Product Analysis and Insight into the Mechanochemical Destruction of Anionic PFAS with Potassium Hydroxide, *J. Hazard. Mater. Adv.*, 2021, 3, 100014.
- 22 K. Gobindlal, Z. Zujovic, P. Yadav, J. Sperry and C. C. Weber, The Mechanism of Surface-Radical Generation and Amorphization of Crystalline Quartz Sand upon Mechanochemical Grinding, *J. Phys. Chem. C*, 2021, 125, 20877–20886.
- 23 G. Cagnetta, J. Robertson, J. Huang, K. Zhang and G. Yu, Mechanochemical destruction of halogenated organic pollutants: a critical review, *J. Hazard. Mater.*, 2016, 313, 85–102.
- 24 P. Roesch, C. Vogel and F. G. Simon, Reductive defluorination and mechanochemical decomposition of per- and polyfluoroalkyl substances (PFASs): from present knowledge to future remediation concepts, *Int. J. Environ. Res. Public Health*, 2020, 17, 1–22.
- 25 L. P. Turner, B. H. Kueper, D. J. Patch and K. P. Weber, Science of the Total Environment Elucidating the relationship between PFOA and PFOS destruction, particle size and electron generation in amended media commonly found in soils, *Sci. Total Environ.*, 2023, 888, 164188.
- 26 L. P. Turner, B. H. Kueper, K. M. Jaansalu, D. J. Patch, N. Batty, O. El-Sharnouby, K. G. Mumford and K. P. Weber, Mechanochemical remediation of perfluorooctanesulfonic acid (PFOS) and perfluorooctanoic acid (PFOA) amended sand and aqueous film-forming foam (AFFF) impacted soil by planetary ball milling, *Sci. Total Environ.*, 2021, 765, 142722.
- 27 N. J. Batty, D. J. Patch, D. M. D. Roberts, N. M. O'Connor, L. P. Turner, B. H. Kueper, M. E. Hulley and K. P. Weber, Use of a horizontal ball mill to remediate per- and polyfluoroalkyl substances in soil, *Sci. Total Environ.*, 2022, 835, 155506.
- 28 N. Yang, S. Yang, Q. Ma, C. Beltran, Y. Guan, M. Morsey, E. Brown, S. Fernando, T. M. Holsen, W. Zhang and Y. Yang, Solvent-Free Nonthermal Destruction of PFAS Chemicals and PFAS in Sediment by Piezoelectric Ball Milling, *Environ. Sci. Technol. Lett.*, 2023, 10, 198–203.
- 29 B. Weiner, L. W. Y. Yeung, E. B. Marchington, L. A. D'Agostino and S. A. Mabury, Organic fluorine content in aqueous film forming foams (AFFFs) and biodegradation of the foam component 6 : 2 fluorotelomermercaptopalkylamido sulfonate (6 : 2 FTSAS), *Environ. Chem.*, 2013, 10, 486–493.
- 30 P. Baláž, *Mechanochemistry in Nanoscience and Minerals Engineering*, Springer-Verlag Berlin Heidelberg, 2008.
- 31 L. Takacs, The historical development of mechanochemistry, *Chem. Soc. Rev.*, 2013, 42, 7649–7659.
- 32 R. J. Cooke, *GEF/UNDP Project on Environmental Remediation of Dioxin Contaminated Hotspots in Vietnam: Independent Expert Evaluation of Three Pilot/Laboratory Scale Technology Demonstrations on Dioxin Contaminated Soil Destruction from the Bien Hoa Airbase in Viet Nam*, Alberta, Canada, 2015.
- 33 U.S. EPA, Combined Mechanical/Chemical Process Removes POPs from Soil and Sediment, *Technol. News Trends*, 2007, vol. 1–6.

